

The Involvement of S100B in Alzheimer's Disease-Related Processes

by

Hayley Naegele

A Thesis Presented in Partial Fulfillment
of the Requirements for the Degree
Master of Science

Approved April 2013 by the
Graduate Supervisory Committee:

Wade McGregor, Chair
Debra Baluch
Wilson Francisco

ARIZONA STATE UNIVERSITY

May 2013

ABSTRACT

Alzheimer's Disease (AD) is the sixth leading cause of death in the United States and the most common form of dementia. Its cause remains unknown, but it is known to involve two hallmark pathologies: Amyloid Beta plaques and neurofibrillary tangles (NFTs). Several proteins have been implicated in the formation of neurofibrillary tangles, including Tau and S100B. S100B is a dimeric protein that is typically found bound to Ca(II) or Zn(II). These experiments relate to the involvement of S100B in Alzheimer's Disease-related processes and the results suggest that future research of S100B is warranted. Zn(II)-S100B was found to increase the rate at which tau assembled into paired helical filaments, as well as affect the rate at which tubulin polymerized into microtubules and the morphology of SH-SY5Y neuroblastoma cells after 72 hours of incubation. Zn(II)-S100B also increased the firing rate of hippocampal neurons after 36 hours of incubation. Together, these results suggest several possibilities: Zn(II)-S100B may be a key part of the formation of paired helical filaments (PHFs) that subsequently form NFTs. Zn(II)-S100B may also be competing with tau to bind tubulin, which could lead to an instability of microtubules and subsequent cell death. This finding aligns with the neurodegeneration that is commonly seen in AD and which could be a result of this microtubule instability. Ultimately, these results suggest that S100B is likely involved in several AD-related processes, and if the goal is to find an efficient and effective therapeutic target for AD, the relationship between S100B, particularly Zn(II)-S100B, and tau needs to be further studied.

TABLE OF CONTENTS

	Page
LIST OF TABLES.....	iv
LIST OF FIGURES	v
CHAPTER	
1 INTRODUCTION.....	1
2 METHODS.....	21
Tau Protein Expression and Purification	21
S100B Purification	22
PHF Formation Assay	23
Tubulin Polymerization Assay	23
Cell Culture	24
SH-SY5Y Cell Imaging	25
Firing Rate Analysis.....	25
3 RESULTS.....	27
PHF Formation Assay	27
Tubulin Polymerization Assay	28
SH-SY5Y Cell Imaging	29
Firing Rate Analysis.....	29
4 DISCUSSION	31
PHF Polymerization Assay	31
Tubulin Polymerization Assay	32

SH-SY5Y Cell Imaging	33
Firing Rate Analysis.....	34
REFERENCES	36

LIST OF TABLES

Table	Page
1. Samples for cell culture and S100B imaging	25

LIST OF FIGURES

Figure	Page
1. Structure of a typical neuron.....	3
2. Hyperphosphorylation and aggregation of tau	4
3. Model for multistep process of tau aggregation.....	11
4. Differential splicing of the tau gene	14
5. PHF polymerization assay	27
6. Tubulin polymerization assay	28
7. SH-SY5Y cell imaging	29
8. Firing rate analysis	30

Chapter 1

INTRODUCTION

Alzheimer's Disease (AD) is the sixth leading cause of death in the United States and the only cause of death among the top ten that cannot be prevented, treated, or cured. It is the most common form of dementia; there were 26.6 million sufferers worldwide in 2006, and it is predicted to affect 1 in 85 people globally by 2050 (Brookmeyer, Johnson, Ziegler-Graham, & Arrighi, 2007). The most commonly recognized symptom is forgetfulness, or the inability to acquire new memories; other symptoms include confusion, mood swings, aggression and irritability and long-term memory loss (Waldemar et al., 2007). There is no cure for AD, and although the goal of treatment is to slow the progression of the disease, this has proven very difficult.

Generally, AD affects the cerebral cortex, specifically in the parietal and temporal lobes, and the hippocampus, which is located in the medial temporal lobe. (Wenk, 2003). The cerebral cortex as a whole plays a key role in memory, attention, perceptual awareness, thought, and language (Shipp, 2007). The parietal and temporal lobes are association areas, which function to produce a perceptual experience of the world, enable people to interact with one another, and support abstract thinking and language. The parietal lobe integrates sensory information from different modalities and helps determine spatial sense and navigation (Fogassi & Luppino, 2005). The temporal lobe is involved in auditory perception as well as processing semantics in both speech and vision. It also contains the hippocampus and plays a key role in the formation of long-term memory (Squire, Stark, & Clark, 2004).

Neurons are electrically excitable cells that process and transmit information by electrical and chemical signaling and they require specialized connections, called synapses, with other neurons that they use for communication. Neurons normally connect to one another to form neural networks; this is how signals are received from the brain and spinal cord and transmitted to glands, muscles, and other parts of the body. There is a wide variety in shape, size, and electrochemical properties of neurons, but all share the same basic structure (Figure 1). The cell body is the central part of the neuron, and it contains the nucleus of the cell. The dendrites of a neuron are cellular extensions that may have many branches; this is where the majority of input to the neuron occurs. The axon is the finer, cable-like projection that extends much further than the dendrites that carries nerve signals away from the cell body. Most neurons have only one axon, but it can become branched in order to enable communication with many target cells. The terminal end of the axon contains synapses, which are specialized structures where neurotransmitters are released to communicate with target neurons. The interconnection of neurons with one another is what forms the pathways for signals to be carried all over the body. When these networks or pathways are interrupted, the electrical or chemical signal carrying the message gets stopped and can't reach its final destination, resulting in a breakdown between the signal the brain receives and the response it intended to trigger.

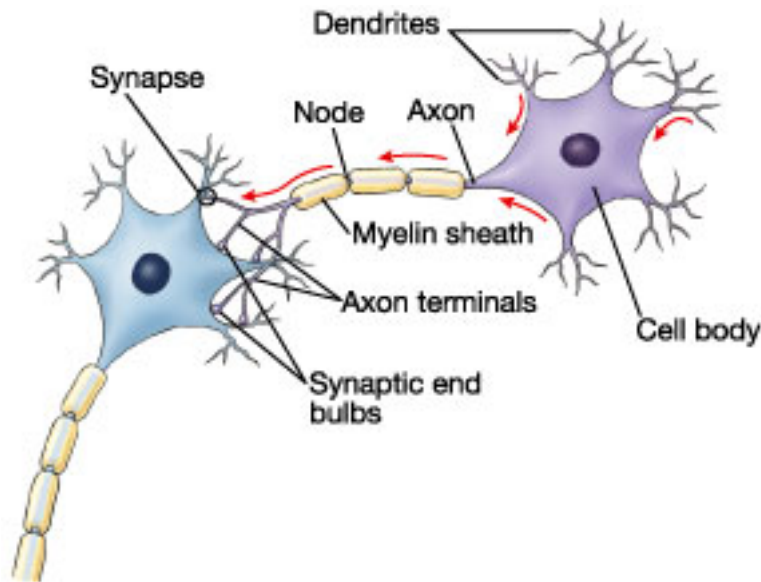


Figure 1. Structure of a typical neuron. (Pearson Education)

The second cell type involved in AD is astrocytes, which are known to perform many functions, including biochemical support of the endothelial cells that form the blood-brain barrier (BBB), provision of nutrients to the nervous tissue, maintenance of extracellular ion balance, and a role in the repair and scarring process of the brain and spinal cord after traumatic injuries (Felts & Smith, 1996). Astrocytes are star-shaped glial cells that exist primarily in the brain and spinal cord, and they are the most abundant cell in the human brain. They are closely associated with neurons, and have many processes that envelope neuronal synapses. In this way, they help regulate the transmission of electrical impulses within the brain.

Learning and memory are induced by a process termed synaptic plasticity, which is the modulation of the strength of synaptic connections between neurons in the brain (Owen & Brenner, 2012). This modulation can be a response to either use or disuse of transmission over the synaptic pathways or from the alteration of the number of receptors located on a synapse. The underlying mechanisms that contribute to synaptic plasticity

include changes in the quantity of neurotransmitters released into a synapse and changes in how effectively cells respond to the neurotransmitters. (Gaiarsa, Caillard, & Ben-Ari, 2002).

The cause and progression of AD are not completely understood, but the pathology of the disease is associated with two major findings: amyloid beta ($A\beta$) plaques and neurofibrillary tangles (NFTs) in the brain (Tiraboschi, Hansen, Thal, & Corey-Bloom, 2004). $A\beta$ plaques are extracellular deposits of amyloid in the gray matter of the brain, and are associated with degenerative neural structures and an abundance of microglia and astrocytes. Neurofibrillary tangles (NFTs), on the other hand, are formed from a hyperphosphorylated form of a microtubule-associated protein (MAP), known as tau. NFT formation produces insoluble aggregations of tau that interfere with normal neuronal pathways in the brain (Figure 2, (Mandelkow, 1999)).

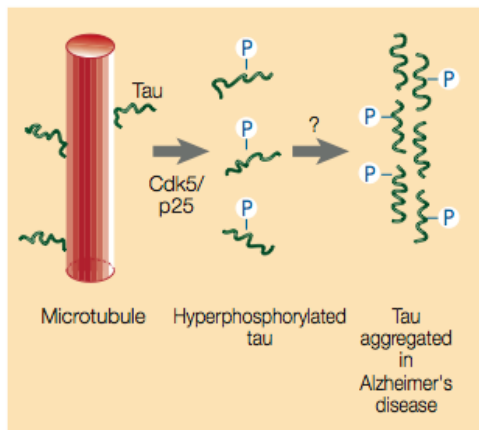


Figure 2. Hyperphosphorylation and aggregation of tau. (Mandelkow, 1999)

Tau is a neuronal MAP found mainly in axons and its main function is to stimulate and stabilize microtubule assembly from tubulin subunits (L. X. Zhou et al., 2007), though it also functions in signal transduction, interaction with the actin cytoskeleton, neurite outgrowth, interactions with the plasma membrane, and the

anchoring of enzymes such as protein kinases and phosphatases (Vladimir N. Uversky, 1998). Tau is primarily active in the distal portions of axons, and is present in dendrites to a lower degree. Microtubules are a main cytoskeletal element in eukaryotic cells and are particularly abundant in nerve cells. Generally, the structure of microtubules is very dynamic and thus requires the stabilization provided by MAPs like tau (Vladimir N. Uversky, 1998). Though somewhat regulated by phosphorylation, hyperphosphorylation of tau proteins can result in MAP dissociation from microtubule, which destabilizes them and leads to tau aggregation into NFTs and paired helical filaments (PHFs). PHFs are aggregations of hyperphosphorylated tau protein that are the components of NFTs. Phosphorylated tau has a “nearly maximal extension and is comparatively stiff” (Hagestedt, Lichtenberg, Wille, Mandelkow, & Mandelkow, 1989), where unphosphorylated tau is highly elastic. Tau is typically highly soluble and survives heat, denaturing agents, and acid treatment without loss of its biological function because it is virtually void of secondary structure (Hagestedt et al., 1989).

In terms of affecting the stability of microtubules, tau can do this via isoforms and/or phosphorylation. The composition of tau is predominantly hydrophilic and charged amino acid residues, and the C-terminal half of tau is what constitutes the microtubule-binding domain (Noble, Pooler, & Hanger, 2011). There are six tau isoforms that exist in brain tissue, three having three binding domains and three having four binding domains. These are a result of alternative splicing of the tau gene.

Phosphorylation of tau is regulated by kinases, including protein kinase N (PKN), and when PKN is activated, it phosphorylates tau, which results in a disruption of the

microtubule organization. Because this increases the pool of insoluble tau, this could be an important first step in generating available protein for the formation of PHFs.

The mechanism by which tau is converted from its water-soluble form into pathogenic insoluble fibrils is not clearly understood, but recently there is increasing evidence to suggest the involvement of zinc. It is well established that the homeostasis of transition metals is altered significantly in AD, with extracellular pooling of zinc and copper in amyloid, and intraneuronal accumulation of iron (Bush, 2012). It has also been shown that zinc released into the brain is needed to maintain memory and cognition (Adlard, Parncutt, Finkelstein, & Bush, 2010). Furthermore, it has been reported that zinc accelerates *in vitro* tau fibrillization, though the mechanism for this is unknown (F. Zhou, Chen, Xiong, Li, & Qu, 2012). In the brain, zinc is released into the synaptic cleft and routinely reaches concentrations of 10-20 μM . It also seems to accumulate in and around NFTs, which are characterized by hyperphosphorylated tau protein, and correlates with the severity of dementia in tauopathies like AD (Religa et al., 2006). It has recently been shown that zinc can accelerate the aggregation of a tau peptide, which is the major protein subunit of a NFT, but it is not known whether or not zinc can trigger the hyperphosphorylation of tau (Mo et al., 2009).

Another protein that has been implicated as a major player in AD and other neurological conditions is S100 calcium binding protein B, or S100B. S100B is a member of the S100 family of proteins, which are proteins that are soluble in nearly saturating (100%) ammonium sulfate and that contain 2 EF-hand motifs that display varying affinities for calcium (Cox, 1998). The EF-hand motif contains a helix-loop-helix topology in which the calcium ions are coordinated by ligands within the loop. Both

EF-hands are flanked by hydrophobic regions at the C and N terminals and are separated by a centrally located hinge region. Generally, S100 proteins are located in the cytoplasm and/or the nucleus of a wide variety of cells, and are involved in the regulation of various cellular processes, including interactions with tubulin and glial fibrillary acidic protein (Smith & Shaw, 1998). S100B is a glial-specific protein that is primarily expressed by astrocytes.

One of S100B's main functions is to enhance the neurite extension of cortical neurons and to stimulate proliferation of glial cells. On the other hand, it also plays a role in the inhibition of protein kinase C (PKC)-mediated phosphorylation, astrocytosis and axonal proliferation, and inhibition of microtubule assembly (Zimmer, Cornwall, Landar, & Song, 1995). It is in the developing central nervous system (CNS) that S100B acts as a neurotrophic factor and induces the survival, development, and function of neurons (Reichardt, 2006). S100B's other functions, including astrocytosis, axonal proliferation, and inhibition of microtubule assembly are thought to occur when S100B is present extracellularly (Zimmer et al., 1995). This diversity of function is accomplished by the ability of S100B to adopt a variety of conformations based on the presence of divalent metal cations, e.g., Ca(II), Zn(II) and Cu(II) (Aimee Landar, 1997). Some activities, such as the enhancement of neurite extension and the proliferation of glial cells, are ascribed to S100B's disulfide-linked dimeric form, in which two monomers, each "formed by two helix-loop-helix EF-hand calcium binding motifs joined by a flexible linker region" are joined (Smith & Shaw, 1998).

In a developing central nervous system, S100B acts as a neurotropic factor as well as a neuronal survival protein. In adults, it is typically elevated in nervous system

damage, making it a potential clinical marker for various conditions, including stroke, concussive brain injury and dementia-related diseases such as AD and Parkinson's (Michetti et al., 2012). Subsequently, S100B has been implicated in AD and other neurological conditions, based on increased levels of the protein in affected brains compared to unaffected brains as well as the fact that the brains of AD patients display evidence of increased oxidative stress, which has been suggested to be related to unregulated redox-active metals in the brain such as copper, iron, and zinc (Hung, Bush, & Cherny, 2010). Although S100B is a calcium-binding protein, it is also known to bind zinc. However, there are currently no indications as to how the S100B dimer is formed *in vivo*.

The tubulin family of proteins, including alpha-tubulin and beta-tubulin, are building blocks for the formation of microtubules. The polymerization of tubulin occurs when dimers of alpha-tubulin and beta-tubulin bind to Guanosine-5'-triphosphate (GTP) and assemble onto the positive ends of microtubules while in the GTP-bound state (Heald & Nogales, 2002). After the dimer becomes incorporated into the existing microtubule, the GTP that remains bound to the beta-tubulin subunit eventually hydrolyzes into Guanosine-5'diphosphate (GDP); the stability of the dimer is affected by whether the beta-tubulin is bound to GTP or GDP. Dimers that are bound to GTP are more readily able to assemble into microtubules, while dimers that are GDP-bound are more likely to fall apart. This cycle is critical to the inherent dynamic instability of microtubules that renders them able to quickly switch between growing and shrinking phases (Howard & Hyman, 2003). It has been shown *in vitro* that S100B modulates this assembly and disassembly of microtubules. In the presence of Ca(II), S100B caused a rapid and nearly

complete disassembly of preformed microtubules in a calcium and pH-dependent manner (Sorci, Agneletti, Bianchi, & Donato, 1998).

Tubulin has also been identified as one of several “best potential targets” for S100B via a consensus sequence. More than 20 proteins that were found to interact in vitro with S100B in a calcium-sensitive manner were screened for the sequence, and those proteins showing a high-match frequency across species were further examined. Tubulin was one of 8 proteins that showed a 100% match. The sequence match indicates an S100B interaction with tubulin domains that would inhibit the polymerization of tubulin (McClintock & Shaw, 2000). It has also been shown that S100 protein (a mixture of S100A and S100B) “exhibits a significant inhibition on tubulin-dependent Ca(II)-ATPase activity of microtubule-associated proteins (MAPs). The ATPase activity in the absence of tubulin, however, was not affected by the S100 protein” (Asai, Miyasaka, Kondo, & Fujii, 1988).

Tau has also been shown to affect tubulin polymerization. In normal cells, tau stabilizes microtubules. In AD, however, tau does not interact properly with microtubules, so they begin to dissociate. Therefore, the tau-microtubule interaction may be an important step on the way to understanding the pathology of AD. It has been shown in several studies that the hyperphosphorylation of tau decreases its affinity for microtubules, which leads to a lack of tau providing the support needed for efficient microtubule assembly. Phosphorylation is the most commonly described post-translational modification of tau, and abnormal phosphorylation occurs before the onset of NFTs (Martin, Latypova, & Terro, 2011). There are at least 85 possible phosphorylation sites on tau and various kinases and phosphatases that regulate the

phosphorylation (Martin et al., 2011). The majority of these phosphorylation sites are serines or threonines, and only a small number are tyrosines. Phosphorylation at all sites has not been studied, but phosphorylation at certain sites has been shown to decrease tau binding to microtubules significantly (Sengupta et al., 1998) and (Dickey et al., 2007).

Furthermore, it has been suggested that tau adopts a state that is reminiscent of PHFs when it is adsorbed to the microtubule surface. While the structure of this state remains unknown, one possibility is that the structure resembles “that of a tau oligomer in a state of aggregation that resembles a PHF nucleus” (Ackmann, Wiech, & Mandelkow, 2000). This would coincide with “the number of tau molecules that are sufficient for PHF nucleation in the presence of polyanions” (Friedhoff, von Bergen, Mandelkow, Davies, & Mandelkow, 1998). Thus, while yet unproven, it remains possible that, *in vivo*, PHF elongation could take place directly on the microtubule surface. Furthermore, the nucleus of this PHF assembly is likely to have a specific structure, which represents yet another possible therapeutic target.

After PHFs have formed, they eventually aggregate into NFTs (figure 7). In non-pathological conditions, tau has been shown to be proteolytically processed by the ubiquitin-proteasome-system (UPS), but in pathological conditions, hyperphosphorylated tau is rendered “less prone to biochemical degradation” and forms PHFs which are subsequently sequestered into NFTs (Martin et al., 2011). Phosphorylation is not the only post-translational modification that may affect the formation of PHFs and NFTs, but it is certainly the most studied.

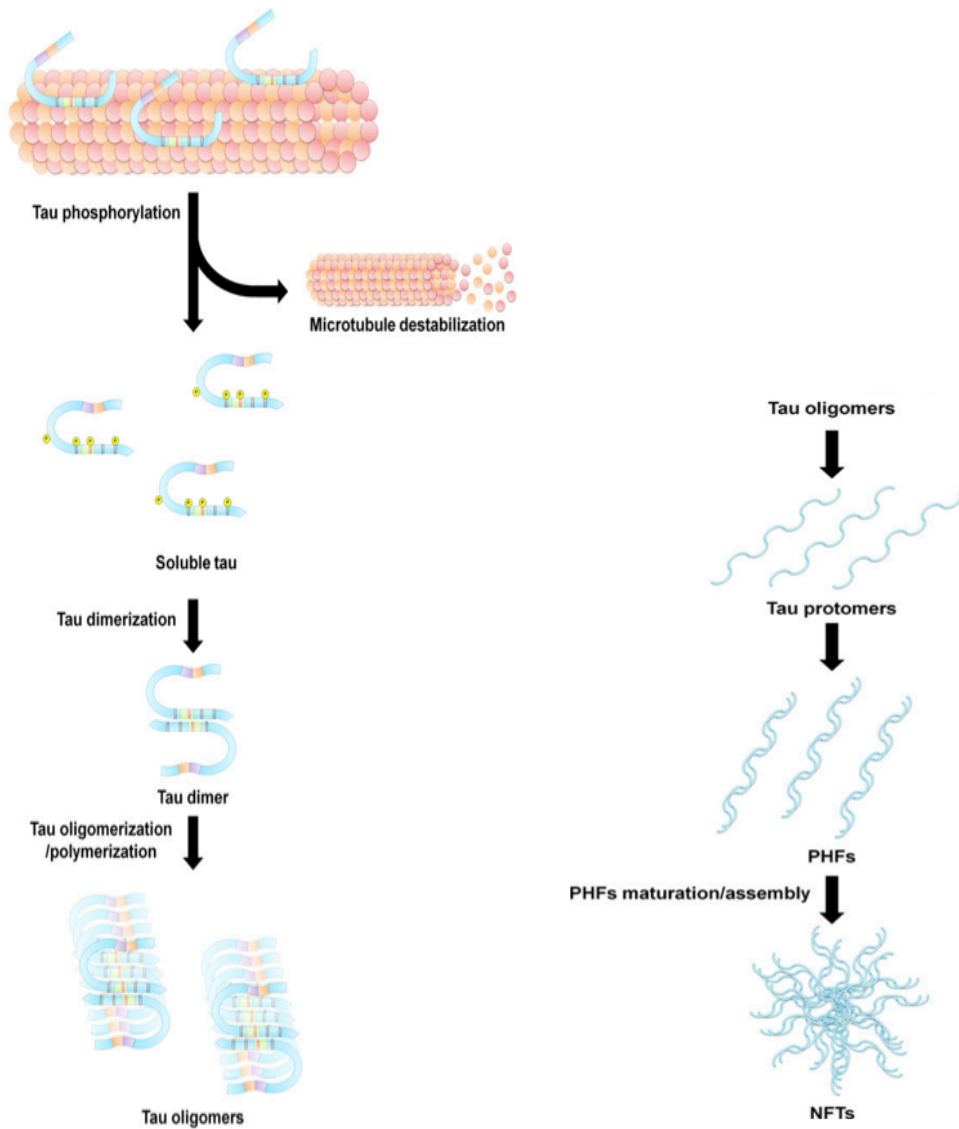


Figure 3. Model for multistep process of tau aggregation

Impairment of tau binding to microtubules results in the increase of monomeric, soluble tau that then dimerizes and assembles into oligomers. The oligomers organize in protomers, which in turn assemble into PHFs and subsequently NFTs. (Martin et al., 2011)

Thus, in the last several decades, it has become clear that targeting tau pathology for the development of therapeutic drugs for AD is not only promising, but necessary. It has already been established that the major biological function of tau is to stimulate

microtubule assembly and to stabilize microtubule structure; this biological activity of tau is regulated by its degree of phosphorylation. Normally, tau in the human brain contains 2-3 moles of phosphate per mole of the protein (Iqbal, Liu, Gong, Alonso Adel, & Grundke-Iqbal, 2009), and hyperphosphorylation of tau depresses its microtubule assembly-promoting activity. It has been seen in the AD affected brain that tau is abnormally hyperphosphorylated and is the major building block of PHFs (Binder, Guillozet-Bongaarts, Garcia-Sierra, & Berry, 2005). This and other abnormal post-translational modifications of tau, including “glycosylation, glycation, prolyl-isomerization, cleavage or truncation, nitration, polyamination, ubiquitination, sumoylation, oxidation, and aggregation” (Martin et al., 2011) are what appear to lead to the neurofibrillary degeneration in AD.

The link between NFTs and neurodegeneration has been shown in several animal models. In one study done in mouse models, it was shown that mis-folded tau proteins induced neurofibrillary degeneration regardless of the difference in the genetic background of the mice (Stozicka et al., 2010). In another, transgenic mice expressing mutant human tau and non-transgenic mice were used to demonstrate a relationship between NFTs and synaptic alterations (Katsuse, Lin, Lewis, Hutton, & Dickson, 2006). In AD and other dementia-related diseases, these synaptic alterations have been emphasized as an important structural correlate, and several studies have suggested that synaptic changes may occur before neuronal loss (DeKosky & Scheff, 1990) and (Terry et al., 1991). Essentially, as tau becomes hyperphosphorylated and aggregates into PHFs, which then aggregate into NFTs, it interferes with the normal neuronal pathways in the

brain, breaking the line of communication from one neuron to another. This breakdown is what leads to the manifested symptoms of AD, such as memory loss and confusion.

Studies of the correlation between pathological changes in the brain and cognitive impairment have demonstrated that the number of NFTs best correlates with the presence or degree of dementia in AD (Iqbal et al., 2009). This provides further evidence that tau plays a critical role in neurodegeneration. Further evidence includes a transgenic mouse model of amyloid pathology and cognitive deficits where tau was knocked out (Iqbal et al., 2009). As a result of the knockout, cognitive deficiencies improved. These, combined with other recent findings on tau, make it clear that targeting tau protein for therapeutic treatments for AD is promising.

Alternative splicing of the tau gene (MAPT) is tissue specific, and there are a total of six isoforms of the tau protein found in the central nervous system (CNS). The six isoforms contain 352-441 amino acids and have molecular weights ranging from 37-46 kDa. Tau proteins in the brain can be described according to four domains, an acidic projection domain at the amino-terminus, a proline-rich region followed by an imperfect microtubule binding repeat motif that is encoded by exons 9-12, and a short carboxy-terminal region. Each isoform of tau is characterized by the length of the N-terminal domain and by the presence of three or four repeat motifs. Diversity of the isoforms is further increased by posttranslational mechanisms, including phosphorylation, O-glycosylation, ubiquitination, nitration, and glycation. One of the isoforms, the shortest, is only expressed in fetal brain, while all six appear in the postnatal period of the human brain (Lee, Goedert, & Trojanowski, 2001). There are 79 potential serine and threonine phosphate acceptor residues in the longest isoform, and phosphorylation at ~30

of these sites has been reported in normal tau proteins (Buee, Bussiere, Buee-Scherrer, Delacourte, & Hof, 2000), and tau phosphorylation is developmentally regulated such that fetal tau is more highly phosphorylated in embryonic CNS than adult CNS. The tau phosphorylation sites are clustered in regions flanking the microtubule binding repeats, and it has been established that increasing tau phosphorylation negatively regulates microtubule binding (Lee et al., 2001). The different isoforms contain different numbers of potential phosphate acceptor residues and can thus be potentially phosphorylated to different degrees, which may relate to their susceptibility to form PHFs.

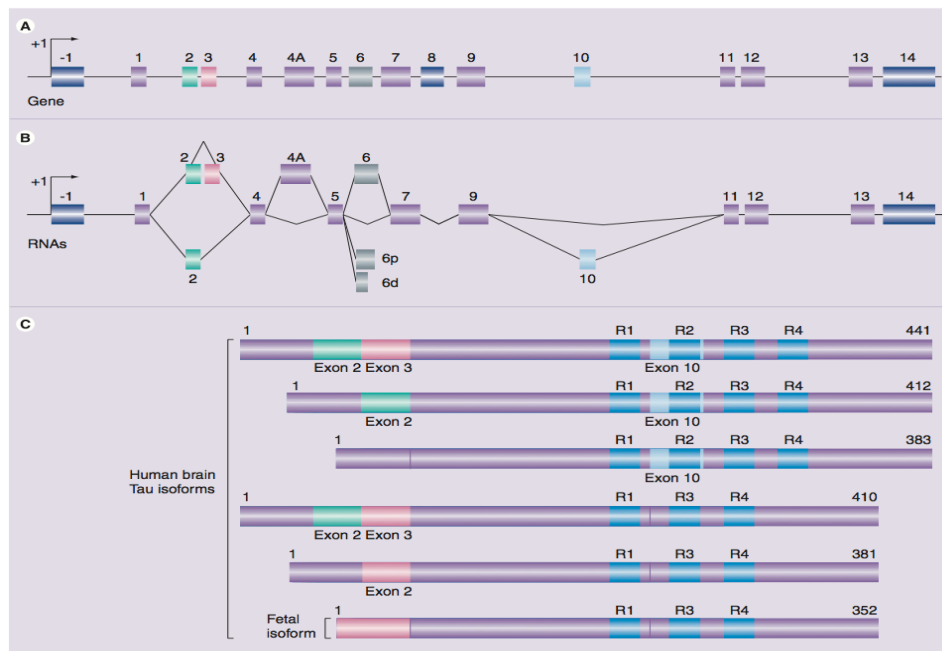


Figure 4. Differential splicing of the tau gene (Sergeant et al., 2008). (A) The tau gene spans more than 130 kb and is composed of 16 exons. (B) Several mRNAs are generated by alternative splicing of exons 2, 3, 4A, and 10. (C) In the brain, six major tau isoforms are generated via alternative splicing.

Hyperphosphorylation of tau has previously been implicated in PHF formation, and there are eighty-five potential phosphorylation sites distributed along a full-length tau molecule (Schraen-Maschke et al., 2008). A high level of phosphorylation on epitopes

that are localized at the half N-terminus and C-terminus outside the microtubule binding domains predominates as the most common posttranslational modification for tau implicated in AD. Normally, the highly basic segments, R3 in 3R tau proteins and R3 and R2 in 4R tau proteins, and the C-terminus interfere with polymerization. Upon hyperphosphorylation, however, tau proteins adopt the conformation needed to polymerize into filaments (Alonso Adel, Mederlyova, Novak, Grundke-Iqbal, & Iqbal, 2004).

Hyperphosphorylation is associated with a loss of microtubule binding capacity and a subsequent accumulation in neuronal bodies, and as such is a relatively early event in the development of AD. Phosphorylated tau also appears to be more resistant to proteolysis by different proteases, which could result in its accumulation in neurons, where it contributes to tau toxicity (Schraen-Maschke et al., 2008). Phosphorylated tau (pTau) has thus been suggested as a predictive biomarker of AD. The rationale is that pTau is known to be a major component of pre-tangle PHF and mature neurofibrillary tangles that are present even before the onset of AD (Schraen-Maschke et al., 2008).

So, while it has been established that hyperphosphorylated tau is likely to lead to PHF formation, the exact mechanism for how this occurs *in vivo* has yet to be discovered. In normal brain, the amino terminal and carboxy terminal flanking regions to the microtubule binding repeats of tau appear to inhibit aggregation into filaments; tau self assembles mainly through the microtubule binding domain/repeat R3 in 3R tau proteins and through R3 and R2 in 4R tau proteins and hyperphosphorylation of tau neutralizes these domains, enabling tau-tau interactions. In AD, however, these regions are

phosphorylated and any native inhibition is eliminated, which results in the formation of PHFs (Iqbal et al., 2009).

In vitro, unphosphorylated tau has been shown to polymerize in the presence of various polyanions, including heparin and arachidonic acid (ARA), and the subsequent structure of PHFs appear to correlate to the structure of AD PHFs when compared via electron microscopy (Stefan Barghorn, 2004) and (Shaun W. Carlson, 2007). Based on the results of polymerization assays, where varying concentrations of tau protein were incubated in the presence of arachidonic acid (ARA) or heparin and polymerization was measured via a fluorescent spectrophotometer, these inducer molecules appear to act as regulatory molecules or allosteric modifiers of the polymerization reaction (Shaun W. Carlson, 2007). It was noted in the same study, that, in the absence of inducer molecules, tau exhibits a very high critical concentration for polymerization. Because there was no spontaneous nucleation, the polymerization of tau has been hypothesized to be more complex than a simple linear polymerization process. The concentration of tau required for polymerization was decreased in the presence of the inducer molecules, suggesting that the same would be true *in vivo*, although what the *in vivo* inducer molecule is, remains unknown.

In a search for the elusive *in vivo* inducer of tau polymerization, it has also been shown that various molecules other than protein kinases bind to tau under different *in vivo* scenarios. In AD, the acidic protein, S100B, is known to bind tau, likely at the basic domain, and potentially cause a change in its ability to be phosphorylated. S100B is a small molecular weight zinc-calcium binding protein that is produced by astrocytes (Yu & Fraser, 2001). It is upregulated by as much as 20-fold in AD and subsequently has

been implicated as a potential target for therapeutic agents if its interaction with tau can be better understood. S100B has been shown to directly affect tau in several ways, one of which is its ability to block PKC phosphorylation at specific sites (Singh, Wang, et al., 1996). The loss of this PKC phosphorylation has been shown to increase the susceptibility of tau to hyperphosphorylation (Singh, Zaidi, Grundke-Iqbal, & Iqbal, 1996), and we know that hyperphosphorylated tau polymerizes into PHFs and subsequently the NFTs that are a hallmark pathology of AD.

The relationship between S100B and tau is also affected by zinc, which is likely attributable to conformational changes of S100B that result in the exposure of a hydrophobic domain that could be a key site for tau binding (Yu & Fraser, 2001). Assessment of the S100B-tau complex has been done via immunoprecipitation of *in vitro* complexes, and the internalization and subcellular distribution of S100B, in neurons, has been studied in neuroblastoma (SH-SY5Y) cells (Yu & Fraser, 2001). The degree of S100B internalization by SH-SY5Y cells was affected by zinc; there was more internalization when zinc was present than when it was not. It was also noted that zinc produced a much more defined colocalization of S100B with tau when the cells were double-labeled with fluorescent tags, suggesting that internalized S100B may be associated with tau and thereby affect tau function and/or phosphorylation. For example, it has been suggested that S100B may provide a scaffolding for tau to stabilize microtubules, which could potentially contribute to the abnormal neuritic dystrophy that is observed in AD (Azmitia, Rubinstein, Strafaci, Rios, & Whitaker-Azmitia, 1995), or that S100B is a modulator of tau phosphorylation and that any changes in their interaction

could be a factor in the AD-related hyperphosphorylation (Sorci, Agneletti, & Donato, 2000)

Thus far, several points have been established which further implicate S100B as an important player in AD. The first of these is the presence of two cysteine residues in S100B that are required for some of its cellular functions. S100B is typically found as a dimer, but appears to have two different conformations, one when free from metal, and two others when bound to Ca(II) or Zn(II) (Aimee Landar, 1997). The implication of this is that the role S100B plays in regulating or affecting tau may be affected by these different conformations; subsequently, this may present a location for a future novel therapeutic target. Mutation of C68 to a valine did not alter S100B effect on the activity of various target proteins, including tau. However, mutation of S100B's other cysteine residue, C84, to serine, resulted in a loss of tau protein modulation (Aimee Landar, 1997). This suggests that C84 participates in the modulation of tau protein by S100B, but not in the modulation of all proteins by S100B.

S100B has been shown to contain acidic calcium and zinc binding domains that are thought to be involved in the interaction of S100B with tau (Baudier & Cole, 1988). The same study established that tubulin has “sequence homology with the acidic region of S100B subunits” (Baudier & Cole, 1988), from which they proposed that the acidic calcium-binding domains were involved in the interaction between S100B and tau. Tau proteins “consist of a half-N-terminal acidic portion followed by a proline-rich region and the C-terminal tail, which is the basic part of the protein” (Kolarova, Garcia-Sierra, Bartos, Ricny, & Ripova, 2012). There has been evidence to suggest that the “self-aggregation of tau into filaments is inhibited by intact N- and C-termini” (Kolarova et al.,

2012), and subsequently any abnormal phosphorylation or other alterations of either the N- or C- terminal “may induce a relaxed structural conformation in the tau molecule” which “allows the self-interaction between these sticky domains in the formation of PHFs” (Kolarova et al., 2012).

The *in vivo* mechanism for how un-phosphorylated tau polymerizes into PHFs needs to be better understood so that therapeutic agents can be developed to target these pathological structures. Thus far, various investigators have established that it is possible to produce PHFs that are structurally equivalent to AD PHFs *in vitro*. However, a molecule has not been identified at elevated levels *in vivo* of AD-afflicted brains that induces tau polymerization at a rate comparable to the known *in vitro* inducers, heparin and arachidonic acid. Furthermore, cell culture studies have shown that various small molecules, including S100B, can enter various types of cells through the plasma membrane by an unknown mechanism, but this has not been shown *in vivo*.

A tau polymerization assay has been developed, using heparin as an inducer and other polyanions like S100B may also serve as inducers. The objective of this study was to determine the optimum ratio of S100B to tau, to see if S100B might logically be proposed as a physiological inducer of PHF formation. In order to do this, an assay was employed that involved incubating purified tau protein at a range of concentrations with known inducer molecules heparin and arachidonic acid at varying concentrations (Shaun W. Carlson, 2007). Polymerization rate of tau was then measured as a function of the fluorescence generated by a thioflavin-S (ThS) dye molecule that binds only to the polymerized version of tau. The same range of tau protein concentrations was then incubated under the same conditions with the inclusion of zinc-loaded S100B at a range

of concentrations. S100B is a candidate for the currently unknown *in vivo* inducer of PHF formation, because it is up-regulated 20-fold in AD and because it has been established that zinc-loaded S100B can affect the activity of tau. The rate of polymerization of tau as a function of heparin, arachidonic acid or Zn(II)-S100B was measured with the Thioflavin-S fluorescence assay and the kinetics of the different inducers was compared.

Establishing S100B as a potential inducer molecule for PHF formation is one step toward identifying a potential therapeutic target for AD.

Chapter 2

METHODS

Tau Protein Expression and Purification

Tau protein was first expressed in the *Escherichia coli* (*E. coli*) strain BL21, as described by (Barghorn, Biernat, & Mandelkow, 2005). The solution containing the bacteria was then centrifuged and the supernatant removed, resulting in a bacterial pellet. The bacterial pellet was then resuspended in cold resuspension buffer (20 mM MES, 1 mM EGTA, 0.2 mM MgCl₂, 5 mM dithiothreitol (DTT), 1 mM phenylmethylsulfonylfluoride (PMSF), 10 ug/mL leupeptin, 2 mM benzamidin, 10 ug/mL pepstatin A, pH 6.8). The cells were disrupted by 3 rounds of sonication for 30 seconds each round. Then, NaCl was added to a final concentration of 500 mM and the mixture was boiled for 20 minutes. The denatured proteins and cell debris were pelleted at 20,000g for 40 minutes at 4°C, and the supernatant was put into dialysis tubings (3.5 kDa molecular weight cut-off) and dialyzed overnight in cation exchange chromatography buffer A, which consisted of the following: 20 mM MES, 50 mM NaCl, 1 mM EGTA, 1 mM MgCl₂, 2 mM DTT (freshly added), and 0.1 mM PMSF (freshly added), pH 6.8. The dialysate was centrifuged at 20,000g for 40 minutes at 4°C, and the clear supernatant was applied to a cation-exchange chromatography column. Unspecific proteins were washed out with cation exchange chromatography buffer A until the UV-absorption reached a stable value. The tau protein was then eluted with a linear gradient of 60% final concentration of cation exchange chromatography buffer B, which consisted of 20 mM MES, 1 M NaCl, 1 mM EGTA, 1 mM MgCl₂, 2 mM DTT (freshly added), 0.1 mM PMSF (freshly added), pH 6.8 and fractionated. Samples thought to contain tau had

aliquots removed and analyzed by SDS-PAGE. To do this, samples were mixed with SDS-sample buffer and separated on a 15% SDS-PAGE gel and then stained with Coomassie blue. In addition to the samples, a control tau protein from a previous preparation was run for comparison. Samples containing tau were then pooled and concentrated by ultrafiltration. The protein concentration of the final product was determined by spectrophotometry; a dilution of the samples was made and its absorption measured at 280 nm. Then, the extinction coefficient of $7,700 \text{ cm}^{-1} \text{ M}^{-1}$ was used to calculate the concentration of each sample. (Barghorn et al., 2005).

S100B Purification

S100B expressed in *E. coli* was first grown in 1L of LB media at 37 °C with vigorous shaking. When A600 reached 0.7, 1mM IPTG was added and growth was continued for 3-4 hours. The cells were then harvested by centrifugation, washed one time with 50 mM Tris-HCl, pH 8.00, 5 mM MgCl₂, and stored frozen at -80 °C. Cells were resuspended in a volume of 50 mM Tris-HCl, pH 8.00, 5 mM MgCl₂ equal to 10 times their packed weight, and then disrupted by 3 rounds of sonication for 30 seconds per round. Cell debris was removed by centrifugation for 15 minutes at 10,000 rpm. The supernatant solution was then centrifuged for 2 hours at 38,000 rpm. The supernatant solution was collected and ammonium sulfate was added, with stirring, to bring it to 90% of saturation. After the supernatant was collected, it was redissolved in 25 mM Tris-HCl, pH 8.0, 1 mM EDTA, and 1 mM DTT, and dialyzed overnight against the same buffer.

The dialyzed sample was applied to an anion exchange chromatography column. The column was equilibrated in 100% (v/v) buffer A, which consisted of 25 mM Tris-HCl, pH 8.00, 1 mM EDTA, and 1 mM DTT, and elution was monitored at 280 nm with

a flow rate of 1 mL/min. After 30 minutes, the buffer was changed to 100% (v/v) buffer B, which consisted of 25 mM Tris-HCl, pH 8.00, 1 mM EDTA, 1 mM DTT, and 1 M NaCl. Samples thought to contain S100B had aliquots removed and analyzed by SDS-PAGE. To do this, samples were mixed with SDS-sample buffer and separated on a 15% SDS-PAGE gel and then stained with Coomassie Blue. In addition to the samples, a control S100B protein from a previous preparation was run for comparison. Samples containing S100B were then pooled and concentrated by ultrafiltration. The protein concentration of the final product was determined by spectrophotometry; a dilution of the samples was made and its absorption measured at 280 nm. Then, the extinction coefficient of $1520 \text{ cm}^{-1} \text{ M}^{-1}$ was used to calculate the concentration of each sample. (Smith, et al, 1996)

PHF Formation Assay

Purified, full-length tau protein (tau40) ranging from 0 to 5 μM was incubated with heparin, at a final concentration of 5 μM and 0.1-10 μM apo-S100B and 0.1-10 μM Zn(II)-S100B. All samples also included 20 μM Thioflavin S, a dye molecule that binds only to the polymerized version of tau and thus provided the varying fluorescence by which the experiment was measured. Fluorescence measurements were taken at 440 nm excitation and 510 nm emission at 25 °C. Between readings, the samples were stored at 4 °C.

Tubulin Polymerization Assay

8 μM >99% pure porcine tubulin (Cytoskeleton, Inc.) and 1 mM GTP were incubated with either 0.8 μM tau, 0.476 μM Zn(II)-S100B, 0.476 μM Zn(II)-S100B + 0.8 μM tau or 0.8 μM tau + 0.476 μM Zn(II), as a potential catalyst, at room temperature and

the rate of tubulin polymerization was measured by the change in absorbance at 350 nm over time. (Ennulat, Liem, Hashim, & Shelanski, 1989) and (Lee, et al.)

Cell Culture

A sample of SH-SY5Y cells was obtained as a generous gift from Dr. Michael Sierks, Arizona State University (ASU), and these cells were cultured in T-75 flasks containing a 1:1 mixture of Modified Eagle's Medium and Ham's F-12 (Irvine Scientific), supplemented with 10% Fetal Bovine Serum (Irvine Scientific), 1% antibiotic-antimycotic (Irvine Scientific), and 1% amino acids for MEM (Irvine Scientific). Cells were grown at 37 °C and 5% CO₂, and passaged at 70-80% confluence.

After incubating with the experimental media for 24 or 72 hours, cells were plated on glass coverslips coated with a solution made from 2 mL sterile water, 200 µL collagen (400 µg/mL stock solution), 40 µL Poly D-Lysine (1 mg/mL stock solution) in 24-well plates at a density of 0.05×10^6 in 1 mL of complete media. 24 hours later, all *trans*-retinoic acid was added to each well to a final concentration of 10 µM. Differentiation continued for 5 days, at which point the media was removed, and complete media was added back to each well. The experimental conditions were then added to each well, as seen in Table 1. After 24 or 72 hours, the cells were fixed in 2% paraformaldehyde for 15 minutes, followed by permeabilization in 2% paraformaldehyde and 1% Tween20 in Intracellular Buffer (ICB, which consisted of 200 mM Hepes, 50 mM EGTA, 50 mM MgCl₂ and 100 mM KCl) for 15 minutes. Cells were washed in 1X ICB for ten minutes, three times. Primary antibody (Santa Cruz Biotechnology, S-100 # chain (N-15)) was diluted 1:200 as recommended by the manufacturer and 200 µL were added to each well. The cells were incubated overnight at 4 °C on a rotary shaker, followed by another three

washes of ten minutes each in 1X ICB. Secondary antibody (Santa Cruz Biotechnology, d anti-goat IgG-FITC) was diluted 1:500 as recommended by the manufacturer and 200 uL of this solution were added to each well. The cells were incubated again overnight at 4 °C on a rotary shaker, followed by another three washes of ten minutes each in 1x ICB. The coverslips were then removed from the wells, mounted on microscope slides, sealed with clear nail polish and allowed to dry before being imaged.

Sample	Contents (all samples had a total volume of 1 mL)
1	SH-SY5Y cells + ddH2O
2	SH-SY5Y cells + 0.5 μM EDTA
3	SH-SY5Y cells + 0.5 μM S100B + 0.5 μM EDTA
4	SH-SY5Y cells + 0.5 μM Zn(II)-S100B
5	SH-SY5Y cells + 5.0 μM S100B + 5.0 μM EDTA
6	SH-SY5Y cells + 5.0 μM Zn(II)-S100B

Table 1. Samples for cell culture and S100B imaging. All samples were plated at the same density (0.05×10^6 cells/well) and had experimental conditions and culture media added to a final volume of 1 mL

SH-SY5Y Cell Imaging

SH-SY5Y cells were plated at a density of 0.05×10^6 cells/well in a 24 well plate and incubated with a range of concentrations (0.5-5 μM) of apo-S100B and Zn(II)-loaded S100B as well as controls of 0.5-5 μM S100B + EDTA. All experimental conditions and culture media were added to a final volume of 1 mL. After 24 or 72 hours, each sample was fixed and attached to a microscope slide and imaged on a Nikon Video Microscope after 24 or 72 hours of incubation (Table 1).

Firing Rate Analysis

Hippocampal neurons were seeded at a density of 60,000/mm² on two separate microelectrode arrays (MEA), produced and provided by Dr. Jitendran Mathuswamy,

ASU, and the cells were grown for 5-6 days (Khraiche and Muthuswamy, 2012). Both samples had 0.5 μM S100B added to the media, and their neuronal activity was monitored for 10 minutes to obtain a baseline level of activity monitored via the number of spikes per second by a multichannel recording system. Then, 0.5 μM EDTA was added to one sample and 0.75 μM Zn(II) was added to the other and the samples were incubated for 36 hours at 37 °C and 5% CO₂. S100B has a dissociation constant for Zn(II) ranging from 10⁻⁸ – 10⁻⁶ M, which is rather high and indicates a very tight binding interaction between the two (Baudier & Gerard, 1983). Thus, it can be assumed that the Zn(II) did in fact bind to the S100B prior to the recording of activity at 36 hours post incubation. The activity of the neurons on the microelectrodes was then monitored for another ten minutes after the 36 hours of incubation with the use of the same multichannel recording system. Each MEA had 16 recording electrodes, and each electrode's data was recorded separately.

RESULTS

PHF Assay

The PHF assay showed an increase of ThS fluorescence from days 1-4 post-incubation, and a drop in fluorescence between days four and five for the samples containing 50 μM tau incubated with 10 μM ThS and 0.476 μM Zn(II)-S100B or 50 μM tau incubated with 10 μM ThS and 5 μM heparin. The sample with S100B showed a higher level of fluorescence overall, suggesting that the tau assembled into PHFs at a faster rate in the presence of the Zn(II)-S100B than it did in the presence of heparin alone. Samples containing 50 μM tau incubated with 10 μM ThS showed little change in absorbance over the five day period (Figure 5).

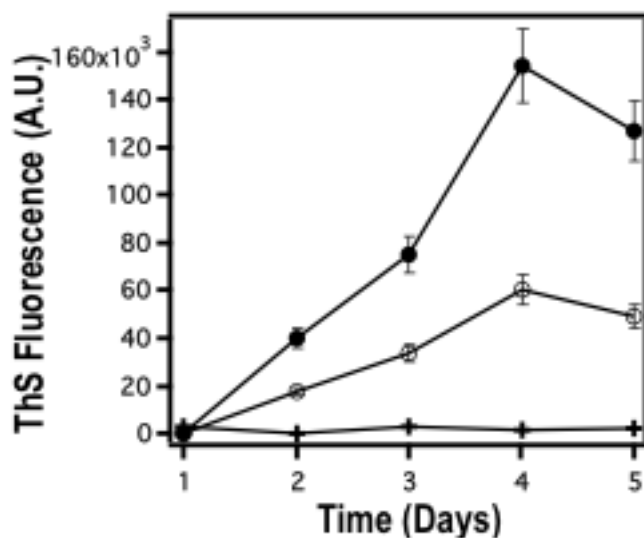


Figure 5. PHF Formation Assay 50 μM tau40 incubated with 10 μM ThS and: no heparin or S100B (crosses), 5 μM heparin (open circles) or 0.476 μM Zn(II)-S100B (closed circles).

Tubulin Polymerization Assay

In the tubulin polymerization assay, absorbance (measured at 350 nm) of samples containing 8 μM tubulin incubated with 1 mM GTP and 0.8 μM tau, 8 μM tubulin incubated with 1 mM GTP and 0.476 μM Zn(II)-S100B, 8 μM tubulin incubated with 1 mM GTP and 0.476 μM Zn(II)-S100B and 0.8 μM tau and 8 μM tubulin incubated with 1 mM GTP and 0.8 μM tau and 0.476 μM Zn(II) increased over time from 0-1500 seconds. Sample A had a rate of 4.29 nM/sec, which was a much faster rate of PHF formation than samples B (1.39 nM/sec), C (1.27 nM/sec), and D (0.467 nM/sec). Samples B and C were similar in rate and sample D significantly slower. A fifth sample, E, containing only 8 μM tubulin and 1 mM GTP showed negligible change in absorbance over time (Figure 6).

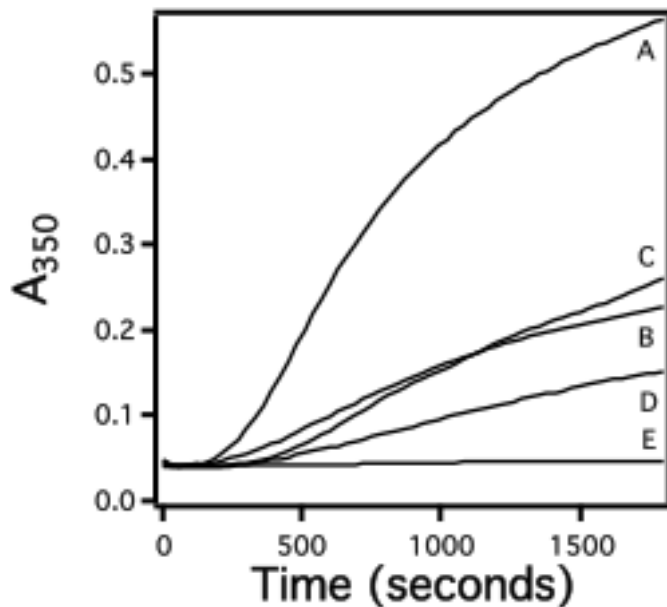


Figure 6. Tubulin polymerization assay. 8 μM tubulin was incubated with 1 mM GTP and with: 0.8 μM tau40 (A), 0.476 μM Zn(II)-S100B (B), 0.476 μM Zn(II)-S100B + 0.8 μM tau40 (C), 0.8 μM tau40 + 0.476 μM Zn(II) (D), and without anything else added (E).

SH-SY5Y Cell Imaging

SH-SY5Y neuroblastoma cells were cultured in the presence of 0.5 or 5.0 μM S100B + EDTA or 0.5 or 5.0 μM Zn(II)-S100B for 24 or 72 hours. Samples incubated with 0.5 μM Zn(II)-S100B showed slight increases in the length of neuritic extensions compared to control cells (without anything added), and samples incubated with 5.0 μM Zn(II)-S100B showed approximately 30% more cell death compared to other samples (Figure 7).

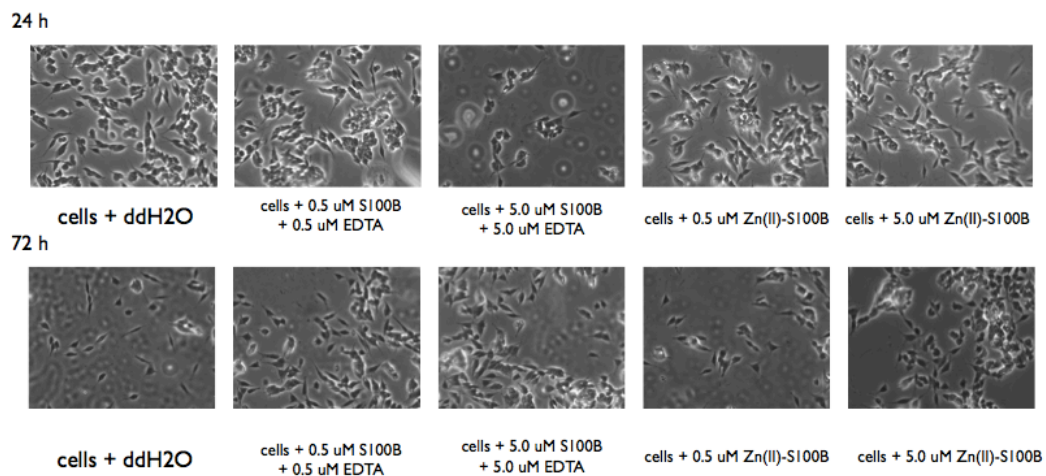


Figure 7. SH-SY5Y Cell Imaging. SH-SY5Y neuroblastoma cell images after 24 and 72 hours.

Firing Rate Analysis

The sample that contained S100B + Zn(II) showed increased firing rate in 15 of the 16 channels present on the MEA, with a greater than 50% increase in firing rate in 14 of those channels. The sample that contained S100B + EDTA showed an increase in firing rate in 9 of 16 channels, with a greater than 50% increase in firing rate in 6 of those channels. (Figure 8.)

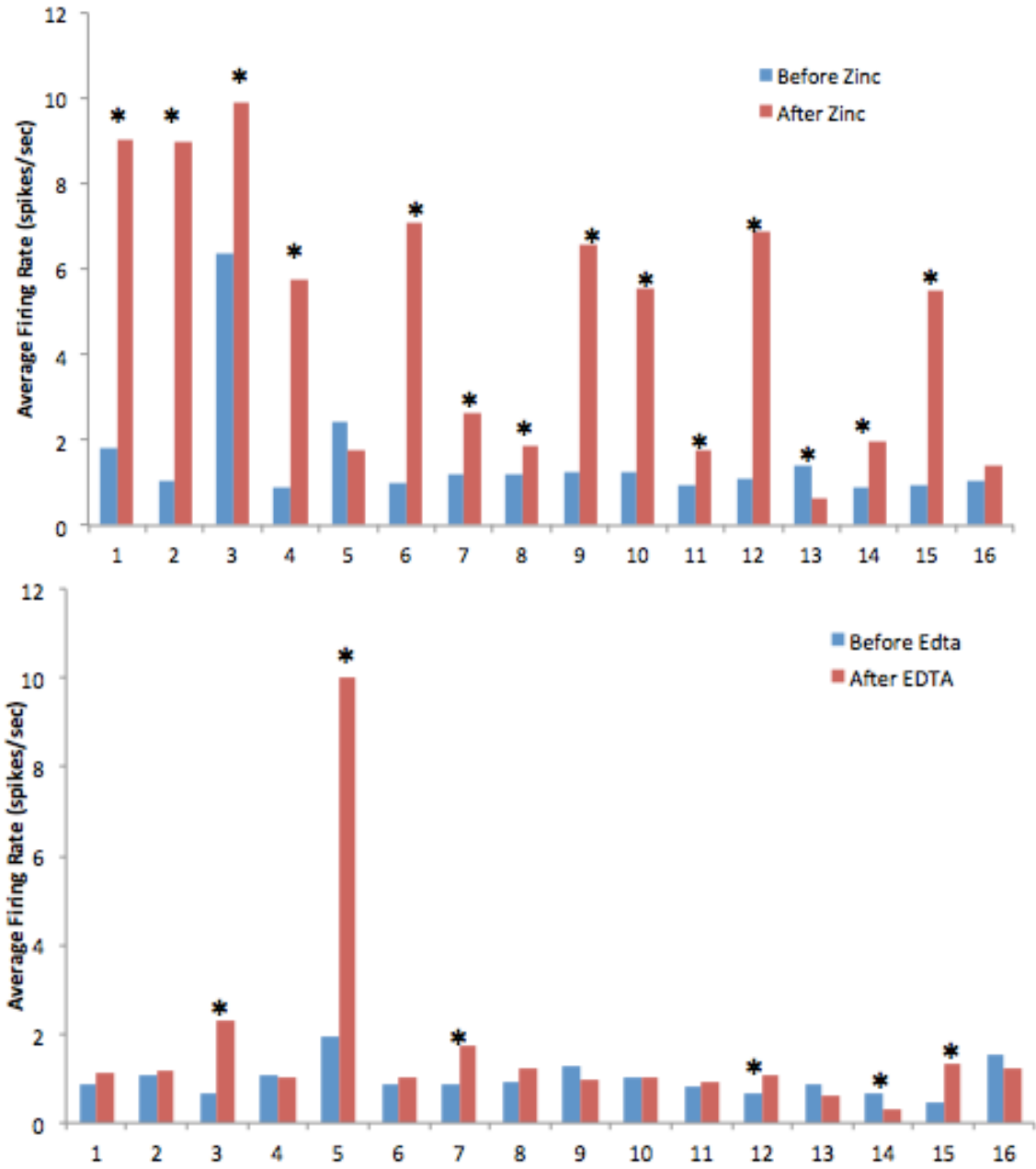


Figure 8. Firing Rate Analysis Activity of neurons after the addition of apo-S100B (blue) and EDTA-S100B (red top) or Zn(II)-S100B (red bottom).

Chapter 4

DISCUSSION

The results of the performed experiments suggest several possible avenues for continued research on the role of S100B in Alzheimer's related processes.

PHF Formation Assay

In the PHF formation assay, samples that contained 50 μM tau incubated with 10 μM ThS and 0.476 μM Zn(II)-S100B or 50 μM tau incubated with 10 μM ThS and 5 μM heparin showed an increase of ThS fluorescence from days 1-4 post-incubation, and a drop in fluorescence between days four and five. The sample that contained S100B showed a higher level of fluorescence overall, suggesting that the tau assembled into PHFs at a faster rate in the presence of the Zn(II)-S100B than it did in the presence of heparin alone. Samples containing 50 μM tau incubated with 10 μM ThS showed little change in absorbance over the five day period (Figure 4). Based on what is already known about S100B, it is likely that it has some effect on tau which affects tau's ability to associate with microtubules, thus creating excess soluble tau that eventually forms PHFs and subsequently NFTs. As discussed previously, S100B contains acidic binding domains that may bind to the basic domain of tau. It has also been reported that "S100B interacts in a Ca(II) and Zn(II) dependent manner with purified tau protein" (Baudier & Cole, 1988). A particular cysteine residue, Cys⁸⁴, which is located in the acidic c-terminal region of S100B and has been implicated in being important in S100B binding target proteins has been shown to be exposed to solvent when S100B is bound to Ca(II) (Landar et al., 1997). When S100B is bound to Zn(II), the same residue is protected due to the

conformation of S100B (Baudier & Cole, 1988). This suggests that metal bound S100B has varying conformations that may affect its binding capabilities. What remains unknown, however, is the mechanism by which all of this occurs. If the mechanism of S100B binding tau could be ascertained, a novel therapeutic target could be developed more easily.

Tubulin Polymerization Assay

The tubulin polymerization assay was designed to further ascertain what effects Zn(II)-S100B may have on microtubules. The sample containing 8 μM tubulin incubated with 1 mM GTP and 0.8 μM tau showed the fastest rate of polymerization at 4.29 nM/sec, while samples containing 8 μM tubulin and 0.476 μM Zn(II)-S100B or 8 μM and 0.476 μM Zn(II)-S100B + 0.8 μM tau40 showed a slower, but similar rate of polymerization (1.39 nM/sec and 1.27 nM/sec respectively) and the sample containing 8 μM tubulin and 0.8 μM tau40 + 0.476 μM Zn(II) showed a further decreased rate of polymerization (0.467 nM/sec). The control sample, which contained only 8 μM tubulin and 1 mM GTP showed no polymerization. These results suggest that the addition of Zn(II)-S100B slows down the rate at which tubulin can polymerize into microtubules. What was of interest was that the sample that contained tubulin and Zn(II)-S100B, but no tau, polymerized at a similar rate to the sample that contained tubulin, Zn(II)-S100B and tau. It may have been expected that the sample containing tau would have a faster polymerization rate than the sample without tau, based on tau's normal functionality as it relates to tubulin polymerization and the stability of resulting microtubules. Instead, these results suggest that the tau that was present may have been affected by the Zn(II)-S100B

that was also present and was subsequently unable to perform its normal functions. However, as discussed regarding the PHF formation assay, the mechanism for how S100B affects tau still remains unknown. These results provide evidence that Zn(II)-S100B affects tau, but we do not know precisely how. It was previously discussed that studies have shown evidence of Ca(II)-S100B inhibiting tubulin polymerization, which underscores the significance of the metal-bound state of S100B toward its physiological function. Zn(II)-S100B, on the other hand, appears to be stimulating tubulin polymerization and these data suggest that tau may be competing with Zn(II)-S100B for the same binding site on tubulin. If this is the case, then the presence of Zn(II)-S100B in AD could be of critical importance. It has already been discussed that it appears to be metal bound S100B that is physiologically significant, and these data support that notion. It is known that zinc levels in the brain are elevated in AD (Bjorklund et al, 2012), which could shift the equilibrium levels of S100B to more of its zinc-bound state in AD. While the activity of Zn(II)-S100B catalyzed tubulin polymerization is lower than the activity catalyzed by tau, there is so much more Zn(II)-S100B present in AD, which could explain the increase in neuritic extensions observed in the SH-SY5Y cells incubated with similar concentrations of Zn(II)-S100B. It is also known that the conformations of Ca(II)-S100B and Zn(II)-S100B are different, and thus may have different affinities for or capabilities of binding to various target proteins. If Zn(II)-S100B binds to tubulin in a similar manner to tau and thus the two compete, it could have important implications for designing a therapeutic target that affects neurofibrillary tangles.

SH-SY5Y Imaging

In an effort to characterize the effect of S100B on the morphology of neuronal cells, SH-SY5Y cells were cultured in the presence of 0.5 or 5.0 μM tau or 0.5 or 5.0 μM Zn(II)-S100B + tau for 72 hours; samples incubated with tau alone showed little change in morphology over the time period. Samples incubated with 0.5 μM Zn(II)-S100B and tau showed slight increases in the length of neuritic extensions compared to wild type cells, and samples incubated with 5.0 μM Zn(II)-S100B and tau showed excessive cell death (Figure 7). This suggests that there may be a difference in the effect of Zn(II)-S100B and tau on cell morphology based on concentration. In AD, Zn(II)-S100B is found at a concentration of 5 μM , which is the concentration at which excessive cell death was seen as well as the concentration that showed no tubulin polymerization in the aforementioned tubulin polymerization assay. The excessive cell death seen in these results corresponds to the neurodegeneration that is also found in AD, and cell death could relate to disturbances in the equilibrium status of microtubules. If the microtubules are not stable enough to continually support the typical structure of a neuron, it stands to reason that the cells would eventually collapse and die. An exact cause for the neurodegeneration seen in AD has yet to be ascertained, and these results suggest a possible avenue for future research in the area.

Firing Rate Analysis

Finally, in the firing rate analysis, evidence is provided that suggests that Zn(II)-S100B affects the activity of neurons. This is particularly interesting; the firing rate of the neurons was increased when incubated with Zn(II)-S100B for 36 hours, but not when incubated with S100B+EDTA. This suggests that the S100B must be zinc loaded (or

perhaps otherwise loaded with a similar metal) in order to affect the firing rate. Affecting neural firing rate is another possible avenue for therapeutic treatments, and further experiments to characterize the effect that difference concentrations of Zn(II)-S100B may have on the firing rate of neurons would be useful. It has been shown previously that neurites in patients with AD exhibit delays in their firing rate when they have elevated levels of A β plaques (Knowles et al., 1999). It would follow that PHFs and NFTs may cause similar delays in neuron firing rate, but this idea has not yet been studied.

Summary

Results of the experiments reported, herein, support the theory that S100B plays a role in AD. Future research would certainly be warranted in establishing a more concrete relationship between the S100B and tau proteins, particularly what effect S100B has on the phosphorylation of tau and how Zn(II)-S100B stimulates PHF formation without inducing tau phosphorylation. It would also be valuable to determine how Zn(II)-S100B catalyzes tubulin polymerization at the biochemical and cellular levels. This information, coupled with an elucidation of how Zn(II)-S100B influences neuronal activity, could help narrow the focus on how this protein could be targeted for AD therapeutic development.

REFERENCES

- Ackmann, M., Wiech, H., & Mandelkow, E. (2000). Nonsaturable binding indicate clustering of tau on the microtubule surface in a paired helical filament-like conformation. *J Biol Chem*, 275(39), 30335-30343.
- Adlard, P.A., Parncutt, J. M., Finkelstein, D. I., & Bush, A. I. (2010). Cognitive loss in zinc transporter-3 knock-out mice: a phenocopy for the synaptic and memory deficits of Alzheimer's disease? *J Neurosci*, 30(5), 1631-1636.
- Aimee Landar, T. L. H., Emily H. Cornwall, John J. Correia, Alexander C. Drohat, David J. Weber, Danna B. Zimmer. (1997). The role of cysteine residues in S100B dimerization and regulation of target protein activity. *Biochimica et Biophysica Acta*.
- Alonso Adel, C., Mederlyova, A., Novak, M., Grundke-Iqbal, I., & Iqbal, K. (2004). Promotion of hyperphosphorylation by frontotemporal dementia tau mutations. *J Biol Chem*, 279(33), 34873-34881.
- Asai, H., Miyasaka, Y., Kondo, Y., & Fujii, T. (1988). Inhibition of tubulin-dependent ATPase activity in microtubule proteins from porcine brain by S100 protein. *Neurochem Int*, 13(4), 509-516.
- Azmitia, E. C., Rubinstein, V. J., Strafaci, J. A., Rios, J. C., & Whitaker-Azmitia, P. M. (1995). 5-HT1A agonist and dexamethasone reversal of para-chloroamphetamine induced loss of MAP-2 and synaptophysin immunoreactivity in adult rat brain. *Brain Res*, 677(2), 181-192.
- Barghorn, S., Biernat, J., & Mandelkow, E. (2005). Purification of recombinant tau protein and preparation of Alzheimer-paired helical filaments in vitro. *Methods Mol Biol*, 299, 35-51.
- Baudier, J., & Cole, R. D. (1988). Interactions between the microtubule-associated tau proteins and S100b regulate tau phosphorylation by the Ca²⁺/calmodulin-dependent protein kinase II. *J Biol Chem*, 263(12), 5876-5883.
- Baudier, J., & Gerard, D. (1983). Ions Binding to S100 Proteins: Structural Changes Induced by Calcium and Zinc on S100a and S100b Proteins. *Biochemistry*, 22, 3360-3369.
- Binder, L. I., Guillozet-Bongaarts, A. L., Garcia-Sierra, F., & Berry, R. W. (2005). Tau, tangles, and Alzheimer's disease. *Biochim Biophys Acta*, 1739(2-3), 216-223.
- Brookmeyer, R., Johnson, E., Ziegler-Graham, K., & Arrighi, H. M. (2007). Forecasting the global burden of Alzheimer's disease. *Alzheimers Dement*, 3(3), 186-191.

- Buee, L., Bussiere, T., Buee-Scherrer, V., Delacourte, A., & Hof, P. R. (2000). Tau protein isoforms, phosphorylation and role in neurodegenerative disorders. *Brain Res Rev*, 33(1), 95-130.
- Bush, A. I. (2012). The Metal Theory of Alzheimer's Disease. *J Alzheimers Dis*.
- Bjorklund, N.L., Sadagoparamanujam, V.M., Tagliatela, G. (2012). Selective, quantitative measurement of releasable synaptic zinc in human autopsy hippocampal brain tissue from Alzheimer's disease patients. *J Neurosci Methods*, 203(1), 146-151.
- Cox, C. W. H. a. J. A. (1998). New perspectives on S100 proteins: a multi-functional Ca^{2+} -, Zn^{2+} -, and Cu^{2+} - binding protein family. *Biometals*, 11, 383-397.
- DeKosky, S. T., & Scheff, S. W. (1990). Synapse loss in frontal cortex biopsies in Alzheimer's disease: correlation with cognitive severity. *Ann Neurol*, 27(5), 457-464.
- Dickey, C. A., Kamal, A., Lundgren, K., Klosak, N., Bailey, R. M., Dunmore, J., . . . Petrucelli, L. (2007). The high-affinity HSP90-CHIP complex recognizes and selectively degrades phosphorylated tau client proteins. *J Clin Invest*, 117(3), 648-658.
- Ennulat, D. J., Liem, R. K., Hashim, G. A., & Shelanski, M. L. (1989). Two separate 18-amino acid domains of tau promote the polymerization of tubulin. *J Biol Chem*, 264(10), 5327-5330.
- Felts, P. A., & Smith, K. J. (1996). Changes in the distribution of a calcium-dependent ATPase during demyelination and remyelination in the central nervous system. *J Neurocytol*, 25(3), 171-180.
- Fogassi, L., & Luppino, G. (2005). Motor functions of the parietal lobe. *Opin Neurobiol*, 15(6), 626-631.
- Friedhoff, P., von Bergen, M., Mandelkow, E. M., Davies, P., & Mandelkow, E. (1998). A nucleated assembly mechanism of Alzheimer paired helical filaments. *Proc Natl Acad Sci U S A*, 95(26), 15712-15717.
- Gaiarsa, J. L., Caillard, O., & Ben-Ari, Y. (2002). Long-term plasticity at GABAergic and glycinergic synapses: mechanisms and functional significance. [Review]. *Trends Neurosci*, 25(11), 564-570.
- Hagestedt, T., Lichtenberg, B., Wille, H., Mandelkow, E. M., & Mandelkow, E. (1989). Tau protein becomes long and stiff upon phosphorylation: correlation between

- paracrystalline structure and degree of phosphorylation. *J Cell Biol*, 109(4 Pt 1), 1643-1651.
- Heald, R., & Nogales, E. (2002). Microtubule dynamics. *J Cell Sci*, 115(Pt 1), 3-4.
- Howard, J., & Hyman, A. A. (2003). Dynamics and mechanics of the microtubule plus end. *Nature*, 422(6933), 753-758.
- Hung, Y. H., Bush, A. I., & Cherny, R. A. (2010). Copper in the brain and Alzheimer's disease. *J Biol Inorg Chem*, 15(1), 61-76.
- Iqbal, K., Liu, F., Gong, C. X., Alonso Adel, C., & Grundke-Iqbal, I. (2009). Mechanisms of tau-induced neurodegeneration. *Acta Neuropathol*, 118(1), 53-69.
- Katsuse, O., Lin, W. L., Lewis, J., Hutton, M. L., & Dickson, D. W. (2006). Neurofibrillary tangle-related synaptic alterations of spinal motor neurons of P301L tau transgenic mice. *Neurosci Lett*, 409(2), 95-99.
- Khraiche, M., and Muthuswamy, J. (2012). Multi-modal biochip for simultaneous, real-time measurement of adhesion and electrical activity of neurons in culture. *Lab Chip*, 2012, 12, 2930-2941.
- Knowles, R. B., Wyart, C., Buldyrev, S. V., Cruz, L., Urbanc, B., Hasselmo, M. E., Stanley, H.E., Hyman, B. T. (1999). Plaque-induced neurite abnormalities: implications for disruption of neural networks in Alzheimer's disease. *Proc Natl Acad Sci U S A*, 96(9), 5274-5279.
- Kolarova, M., Garcia-Sierra, F., Bartos, A., Ricny, J., & Ripova, D. (2012). Structure and pathology of tau protein in Alzheimer disease. *Int J Alzheimers Dis*, 2012, 731526.
- Landar, A., Hall, T. L., Cornwall, E. H., Correia, J. J., Drohat, A. C., Weber, D. J., & Zimmer, D. B. (1997). The role of cysteine residues in S100B dimerization and regulation of target protein activity. *Biochim Biophys Acta*, 1343(1), 117-129.
- Lee, V. M., Goedert, M., & Trojanowski, J. Q. (2001). Neurodegenerative tauopathies. *Annu Rev Neurosci*, 24, 1121-1159.
- Mandelkow, E. (1999). Alzheimer's disease. The tangled tale of tau. *Nature*, 402(6762), 588-589.
- Martin, L., Latypova, X., & Terro, F. (2011). Post-translational modifications of tau protein: implications for Alzheimer's disease. *Neurochem Int*, 58(4), 458-471.

- McClintock, K. A., & Shaw, G. S. (2000). A logical sequence search for S100B target proteins. *Protein Sci*, 9(10), 2043-2046.
- Michetti, F., Corvino, V., Geloso, M. C., Lattanzi, W., Bernardini, C., Serpero, L., & Gazzolo, D. (2012). The S100B protein in biological fluids: more than a lifelong biomarker of brain distress. *J Neurochem*, 120(5), 644-659.
- Mo, Z. Y., Zhu, Y. Z., Zhu, H. L., Fan, J. B., Chen, J., & Liang, Y. (2009). Low micromolar zinc accelerates the fibrillization of human tau via bridging of Cys-291 and Cys-322. *J Biol Chem*, 284(50), 34648-34657.
- Noble, W., Pooler, A. M., & Hanger, D. P. (2011). Advances in tau-based drug discovery. *Expert Opin Drug Discov*, 6(8), 797-810.
- Owen, G. R., & Brenner, E. A. (2012). Mapping molecular memory: navigating the cellular pathways of learning. *Cell Mol Neurobiol*, 32(6), 919-941.
- Reichardt, L. F. (2006). Neurotrophin-regulated signalling pathways. *Philos Trans R Soc Lond B Biol Sci*, 361(1473), 1545-1564.
- Religa, D., Strozyk, D., Cherny, R. A., Volitakis, I., Haroutunian, V., Winblad, B., Naslund, J., Bush, A. I. (2006). Elevated cortical zinc in Alzheimer disease. *Neurology*, 67(1), 69-75.
- Schraen-Maschke, S., Sergeant, N., Dhaenens, C. M., Bombois, S., Deramecourt, V., Caillet-Boudin, M. L., Pasquier, F., Maurice, C.A., Sablonniere, B., Vanmechelen, E., Buee, L. (2008). Tau as a biomarker of neurodegenerative diseases. *Biomark Med*, 2(4), 363-384.
- Sengupta, A., Kabat, J., Novak, M., Wu, Q., Grundke-Iqbal, I., & Iqbal, K. (1998). Phosphorylation of tau at both Thr 231 and Ser 262 is required for maximal inhibition of its binding to microtubules. *Arch Biochem Biophys*, 357(2), 299-309.
- Sergeant, N., Bretteville, A., Hamdane, M., Caillet-Boudin, M. L., Grognet, P., Bombois, S., Blum, D., Delacourte, A., Pasquier, F., Vanmechelen, E., Schraen-Maschke, S., Buee, L. (2008). Biochemistry of Tau in Alzheimer's disease and related neurological disorders. *Expert Rev Proteomics*, 5(2), 207-224.
- Shaun W. Carlson, M. B., Kellen Voss, Qian Sun, Carolyn A. Rankin, T. Chris Gamblin. (2007). A Complex Mechanism for Inducer Mediated Tau Polymerization. *Biochemistry*, 46, 8838-8849.
- Shipp, S. (2007). Structure and function of the cerebral cortex. *Curr Biol*, 17(12), R443-449.

- Singh, T. J., Wang, J. Z., Novak, M., Kontzekova, E., Grundke-Iqbal, I., & Iqbal, K. (1996). Calcium/calmodulin-dependent protein kinase II phosphorylates tau at Ser-262 but only partially inhibits its binding to microtubules. *FEBS Lett*, 387(2-3), 145-148.
- Singh, T. J., Zaidi, T., Grundke-Iqbal, I., & Iqbal, K. (1996). Non-proline-dependent protein kinases phosphorylate several sites found in tau from Alzheimer disease brain. *Mol Cell Biochem*, 154(2), 143-151.
- Smith, S. P., & Shaw, G. S. (1998). A novel calcium-sensitive switch revealed by the structure of human S100B in the calcium-bound form. *Structure*, 6(2), 211-222.
- Sorci, G., Agneletti, A. L., Bianchi, R., & Donato, R. (1998). Association of S100B with intermediate filaments and microtubules in glial cells. *Biochim Biophys Acta*, 1448(2), 277-289.
- Sorci, G., Agneletti, A. L., & Donato, R. (2000). Effects of S100A1 and S100B on microtubule stability. An in vitro study using triton-cytoskeletons from astrocyte and myoblast cell lines. *Neuroscience*, 99(4), 773-783.
- Squire, L. R., Stark, C. E., & Clark, R. E. (2004). The medial temporal lobe. *Annu Rev Neurosci*, 27, 279-306.
- Stefan Barghorn, J. B., and Eckhard Mandelkow. (2004). Purification of Recombinant Tau Protein and Preparation of Alzheimer-Paired Helical Filaments In Vitro. *Methods in Molecular Biology*, 299, 35-51.
- Stozicka, Z., Zilka, N., Novak, P., Kovacech, B., Bugos, O., & Novak, M. (2010). Genetic background modifies neurodegeneration and neuroinflammation driven by misfolded human tau protein in rat model of tauopathy: implication for immunomodulatory approach to Alzheimer's disease. *J Neuroinflammation*, 7, 64.
- Terry, R. D., Masliah, E., Salmon, D. P., Butters, N., DeTeresa, R., Hill, R., Hansen, L.A., Katzman, R. (1991). Physical basis of cognitive alterations in Alzheimer's disease: synapse loss is the major correlate of cognitive impairment. *Ann Neurol*, 30(4), 572-580.
- Tiraboschi, P., Hansen, L. A., Thal, L. J., & Corey-Bloom, J. (2004). The importance of neuritic plaques and tangles to the development and evolution of AD. *Neurology*, 62(11), 1984-1989.
- Vladimir N. Uversky, S. W., Oxana V. Galzitskaya, Leonhard Kittler, Gunter Lober. (1998). Hyperphosphorylation induces structural modification of tau-protein. *FEBS*, 439, 21-25.

- Waldemar, G., Dubois, B., Emre, M., Georges, J., McKeith, I. G., Rossor, M., Scheltens, P., Tariska, P., Winblad, B. (2007). Recommendations for the diagnosis and management of Alzheimer's disease and other disorders associated with dementia: EFNS guideline. *Eur J Neurol*, 14(1), e1-26.
- Wenk, G. L. (2003). Neuropathologic changes in Alzheimer's disease. [Review]. *J Clin Psychiatry*, 64 Suppl 9, 7-10.
- Yu, W. H., & Fraser, P. E. (2001). S100B Interaction with Tau is Promoted by Zinc and Inhibited by Hyperphosphorylation in Alzheimer's Disease. *The Journal of Neuroscience*, 21, 2240-2246.
- Zhou, F., Chen, S., Xiong, J., Li, Y., & Qu, L. (2012). Luteolin Reduces Zinc-Induced Tau Phosphorylation at Ser262/356 in an ROS-Dependent Manner in SH-SY5Y Cells. *Biol Trace Elem Res*.
- Zhou, L. X., Du, J. T., Zeng, Z. Y., Wu, W. H., Zhao, Y. F., Kanazawa, K., Ishizuka, Y., Nemoto, T., Nakanishi, H., Li, Y. M. (2007). Copper (II) modulates in vitro aggregation of a tau peptide. *Peptides*, 28(11), 2229-2234.
- Zimmer, D. B., Cornwall, E. H., Landar, A., & Song, W. (1995). The S100 protein family: history, function, and expression. [Review]. *Brain Res Bull*, 37(4), 417-429